Journal of Membrane Science 427 (2013) 73–84

Contents lists available at SciVerse ScienceDirect

Journal of Membrane Science

journal homepage: www.elsevier.com/locate/memsci

Preparation and characterization of polyvinyl acetate/zeolite 4A mixed matrix membrane for gas separation

Jamil Ahmad, May-Britt Hägg*

Department of Chemical Engineering, Faculty of Natural Sciences and Technology, Norwegian University of Science and Technology (NTNU), NO-7491 Trondheim, Norway

ARTICLE INFO

Article history:
Received 3 February 2012
Received in revised form
19 September 2012
Accepted 21 September 2012
Available online 28 September 2012

Keywords:
PVAc
Zeolite 4A
MMMs
Thermal stability
Separation properties

ABSTRACT

The demand and consumption of fossil fuels have increased in the past and continue to increase in future. The combustion of these fossil fuels produce various harmful gases i.e CO_2, SO_2, H_2S etc. that pose potential threat to the environment. Currently the development of new membrane materials is the focus of research in membrane based gas separation. Pure PVAc and PVAc/4A mixed matrix membranes were prepared using dichloromethane as a solvent and the solution casing method. The resulting membranes were characterized by optical microscope, FESEM, DSC, TGA, XRD and single gas permeation. Optical microscope was used to find out the initial thickness of membranes that ranges from 70 μm to 90 μm. Zeolite 4A particles upto 35 wt% were homogenously dispersed within the polymer without aggregation as shown by the FESEM results. The addition of 4A particles have improved the thermal stability of PVAc in the resulting MMMs as depicted by an increase in the glass transition temperature (T_g) and TGA results. In single gas permeation, the effects of zeolite 4A loading, operating temperature and pressure on the separation properties were investigated. The obtained results show that the addition of zeolite 4A up to 25 wt% has increased the selectivity of gas pairs O_2/N_2, H_2/N_2 and CO_2/N_2 by 25%, 37% and 70% respectively with a corresponding decrease in their permeability. Temperature increase from 30 °C to 50 °C has a positive effect on permeabilities with a maximum of $(1.19)\times 3.348\times 10^{-19}$ kmol m/(m^2 s Pa) (barrer) for O_2, $(17.55)\times 3.348\times 10^{-19}$ kmol m/(m^2 s Pa) (barrer) for H_2 and $(9.35)\times 3.348\times 10^{-19}$ kmol m/(m^2 s Pa) (barrer) for CO_2 and a negative effect on their selectivity over N_2. As the pressure is increased from $(2)\times 100{,}000$ Pa (bars) to $8\times 100{,}000$ Pa (bars), permeability of H_2 almost remains constant and slightly increases for O_2. Permeability of N_2 and CO_2 is decreased and increased respectively leading to increased selectivity of CO_2/N_2 as well as H_2/N_2 and O_2/N_2. The obtained results are consistent with the reported literature data.

1. Introduction

As a result of industrial activities, CO_2 is produced in mixture with other gases like CH_4, H_2 and N_2. CO_2 in very high concentrations is a gas with serious effects on global warming and should preferably be removed from these gases [1]. The conventional method used for CO_2 removal is by reversible solvent absorption. However this process consumes high amount of energy and is hence cost intensive [2]. The energy efficiency and mechanical simplicity of membrane gas separation make it an economically viable and environmental friendly option for CO_2 capture [3,4]. Membrane gas separation is a dynamic and rapidly growing field. It was started in 1980 when used for hydrogen purification and has grown into a US$150 million/year industry in 2000. Future membrane market is anticipated to reach US$750 million/year by 2020 [5,6].

The discovery of high flux asymmetric phase-inverted membranes in 1962, has led to the rapid development of polymeric membranes. It was applied to gas separation and found suitable for the separation of helium from natural gas [7]. Current applications of membrane-based gas separation include oxygen and nitrogen enrichment, hydrogen recovery, natural gas sweetening (CO_2 removal) and removal of volatile organic compounds from effluent streams. Beside this some small scale applications include H_2S removal from natural gas, water removal from air stream and olefin/paraffin separation [8]. A number of advantages including low capital cost, lower energy requirements, small footprints and ease of operation are offered by membrane separation[9,10]. An upper bound limit for the performance of polymeric membranes in gas separation was predicted by Robeson [11]. This upper bound which is showing a tradeoff between permeability and selectivity represents the biggest challenge for

* Corresponding author. Tel.: +47 73594033; fax: +47 73594080.
E-mail address: may-britt.hagg@chemeng.ntnu.no (M.-B. Hägg).

0376-7388/$ - see front matter © 2012 Elsevier B.V. All rights reserved.
http://dx.doi.org/10.1016/j.memsci.2012.09.036

improved separation performance, and limit their application in industry [8,12]. From 1990 to 2008 different researchers have focused their efforts on tailoring polymer structures for membrane materials and obtained better separation of O_2/N_2 [13,14], CO_2/N_2 [15,16] and H_2/N_2 [17,18]. Inspite of the improvement in gas separation properties it has only slightly shifted the upper bound as shown by Robeson in his revised upper bound in 2008 [19].

Membranes formed from inorganic materials include metallic, ceramics, glass and zeolite membrane and have much higher thermal, chemical and mechanical stability compared to the polymeric membranes [20,21]. For gas separation, membranes of zeolites with various pore sizes are successfully used [22]. Carbon molecular sieve membranes(CMSMs) are produced by the carbonization of a suitable polymer precursor under controlled conditions with excellent gas separation properties [23,24]. However the high cost of membrane production and handling issues due to its brittle nature are the challenges that should be addressed to fully exploit its potential for gas separation [25,26]. The work of Memfo research group at NTNU-Norway is worth-mentioning in this regard [27,28].

New membrane materials composed of polymer as a continuous phase and inorganic as dispersed phase, are called mixed matrix membrane (MMMs) and was first reported when delayed diffusion time lag effect was observed for CO_2 and CH_4 by adding zeolite 5A into rubbery polymer PDMS [29]. Later researchers at the company UOP documented that MMMs might give superior separation properties compared to that of pure polymer [30]. The concept of MMMs was further exploited by different researchers using rubbery polymers and porous inorganic particles. The rubbery polymers owing to their soft and flexible nature adhere to the inorganic particles and successful MMMs were prepared. However few studies showed improvement in the gas separation properties [31]. In most cases the separation properties did not change remarkably [32]. It was due to the intrinsic low selectivity of these polymers and the mismatch of their permeability in comparison to the dispersed phase particles pointed out by Mahajan and Koros [33]. This has encouraged the use of glassy polymers as continuous phase where the high intrinsic selectivity of the polymers can be benefitial in the resulting MMMs. Therefore porous inorganic fillers such as zeolite and CMS were used in glassy polymers and a number of interesting articles were published [34–45]. The MMMs formed from these rigid glassy polymers contained voids at the particle polymer interface due to lack of adhesion, resulting in nonselective permeation [46]. Different methods including the use of plasticizer, priming the fillers, silane coupling agents, maintaining flexibility during membrane formation and using whisker morphology of fillers for better adhesion were used to eliminate the voids and increase the separation properties. Although the voids were reduced, the separation properties did not improve significantly [33,38–40].

As mentioned above that both the rubbery and glassy polymers have their own challenges in achieving the actual goal of MMMs; therefore we have chosen polyvinyl acetate PVAc as a polymer matrix to prepare MMMs. PVAc has a medium glass transition temperature of 35 °C in comparison to PDMS with low $T_g = -123$ °C and polyimide (PI) with high $T_g = 300$ °C. PVAc is expected to avoid the problems associated with the use of soft and rigid polymers. Reported results from literature show that Zeolite 4A has been used as a dispersed phase with PVAc and the resulting MMMs has better adhesion and separation performance for the gas pairs O_2/N_2 and CO_2/CH_4 [33,45]. In the current work, this pair of polymer and particle has been further investigated for its structural and thermal properties as well as for the separation of gas pairs CO_2/N_2 and H_2/N_2 at different operating conditions.

2. Experimental

2.1. Raw materials

PVAc used in our experiments was purchased from Sigma Aldrich that has an average M.wt of 100,000 and density 1.18 g/cm^3. It was provided in the bead shape with hydrophobic nature. Zeolite 4A used as filler in the MMMs possesses an eight-sided aperture with an affective aperture size of 3.8 Å that falls between the approximate molecular diameters of O_2 and N_2. Zeolite 4A used in our experiments was purchased from Advanced Speciality Gas Equipment ASGE with particle size ranging from 1 μm to 5 μm as shown by the SEM results. It was obtained in the powder form having density of 0.5132 g/cm^3 and moisture content of 1.5 wt%. Dichloromethane (DCM) was used as a solvent. The solvent was purchased from Sigma Aldrich in spectrophotometer grade >99.5% pure, stabilized with 50–150 ppm amylene, having density 1.325 g/cm^3 at 25 °C, M.wt 84.93, boiling point 40 °C and a solubility of 13 g/L in water at 20 °C. The low boiling point of DCM secure that it will need relatively shorter time to evaporate from the system and thus avoid sedimentation of the zeolite particles in the resulting MMMs. The structure of PVAc, zeolite 4A and dichloromethane are given in Fig. 1.

2.2. Membrane preparation

The basic idea for the preparation of MMMs is according to the work of Mahajan and. Koros [33]. The composition of solutions is a key parameter to obtain defect free and thinner membrane simultaneously. Reducing the concentration of solution can help to improve spreading and casting of the solution, but leads to more sedimentation of the zeolite particles resulting in a non-homogenous MMM. On the other hand increasing the concentration can reduce the rate of sedimentation of zeolite particles but the obtained membranes are much thicker with lower permeation. Several compositions were tested out in the laboratory and finally used the optimum to make pure and mixed matrix membranes. For a pure PVAc membrane, 10 wt% polymer in dichloromethane was used. For the MMMs, the solvent with polymer was kept at a fixed amount of 90 wt% and in the remaining 10 wt%, the amount of filler was changed within the range from 15 wt% to 35 wt%. Although membrane with 45 wt% zeolite loading was prepared successfully, it could not be used for

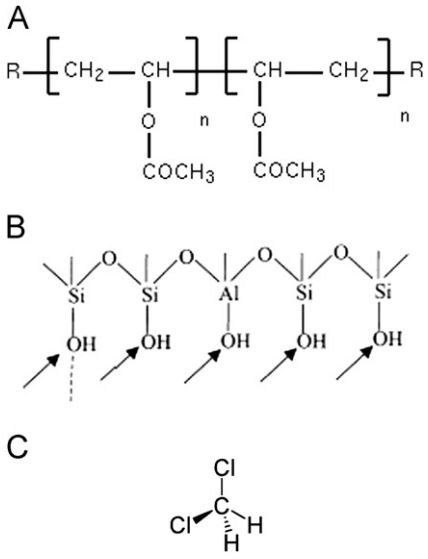

Fig. 1. Structure of (A) PVAc (B) zeolite 4A (C) dichloromethane.

permeation test due to its brittleness. The methodology is shown in Fig. 2. Zeolite 4A powder was first dried in vacuum oven at 200 °C for overnight time. Then a weighted amount from this was taken in a 50 ml scotch flask and mixed with solvent dichloromethane. The solution was sonicated for about 1 min at 60 amplitude without pulsation using ultrasonic processor to disperse the zeolite particles within the solvent. After that PVAc was added and the flask was put on the roller to mix for overnight time. The roller mixer allows slow mixing of the polymer with the zeolite 4A particles. As PVAc stick to glass, the solution was casted on a Teflon plate and leaft there for 24 h to dry by natural evaporation. All the initial membranes formed were defective having bubbles trapped inside and with a nonhomogenous morphology. This was due to the fast evaporation from the membrane surface while still some solvent remained inside. Several modifications were made to solve the problem, however covering the Teflon plate with a pin-holed aluminum foil, putting a glass funnel above it, and keeping tissue paper in its outlet was found successful. This provided a controlled natural evaporation from the surface of the casting solution and defect free membranes were obtained. The membranes were then further dried in a vacuum oven at ambient temperature to remove any residual solvent trapped inside and finally annealed at 50 °C to give additional strength and make it suitable for permeation.

2.3. Membrane characterization

Optical microscope was used to determine the thickness of pure PVAc and MMMs in the range from 70 μm to 90 μm. The cross section and surface morphology of the PVAc and PVAc/4A mixed matrix membranes were examined using field emission scanning electron microscopy (LV FESEM, Zeiss supra, 55VP). The samples were fractured in liquid nitrogen and coated with gold before FESEM analysis. The wide angle X-ray diffraction of PVAc and PVAc/4A MMMs were recorded using Cu Kα radiation of wavelength $\lambda = 1.54$ Å with a graphite monochromator produced by Bruker AXS D8 focus advance X-ray diffraction meter (Rigaku, Japan). The X-ray scans were taken in the 2θ range from 4° to 80° with a scanning speed and step size of 1°/mm and 0.01° respectively to identify any changes in the crystal structure and intermolecular

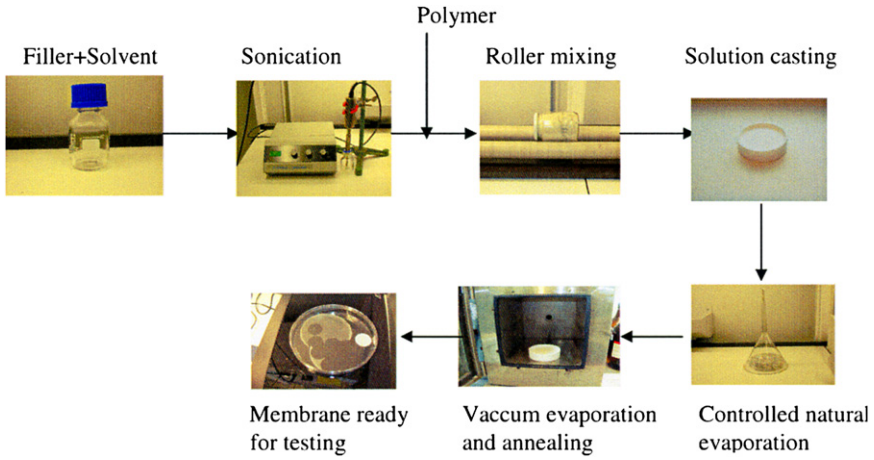

Fig. 2. Laboratory method developed for the preparation of PVAc-4A mixed matrix membrane.

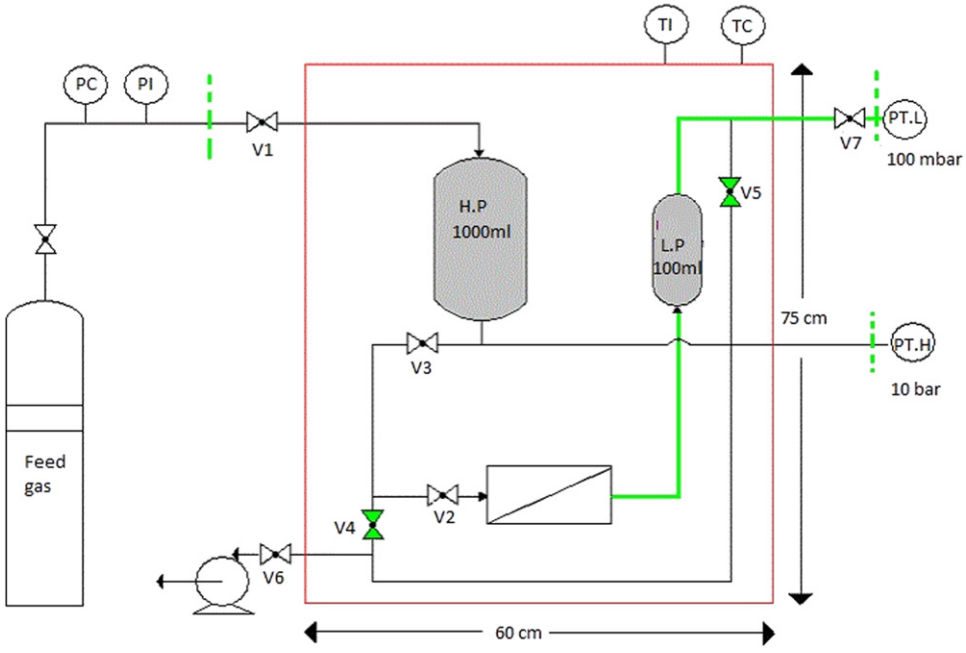

Fig. 3. Permeation setup used for single gas permeation.

distances between inter segmental chains. The thermal properties of PVAc and PVAc/4A MMMs were investigated using TA Q100 differential scanning calorimeter (DSC). The samples were heated from 0 °C to 100 °C under nitrogen atmosphere at a heating rate of 5 °C/min. Thermal stability of PVAc and PVAc/4A MMMs were evaluated by thermogravimetric analyzer TGA (TA Q 500). The TGA measurements were carried out under nitrogen atmosphere over the temperature range of 25–800 °C at a heating rate of 10 °C/min. Separation properties of PVAc and PVAc/4A MMMs were measured with a permeation setup shown in Fig. 3. The membrane

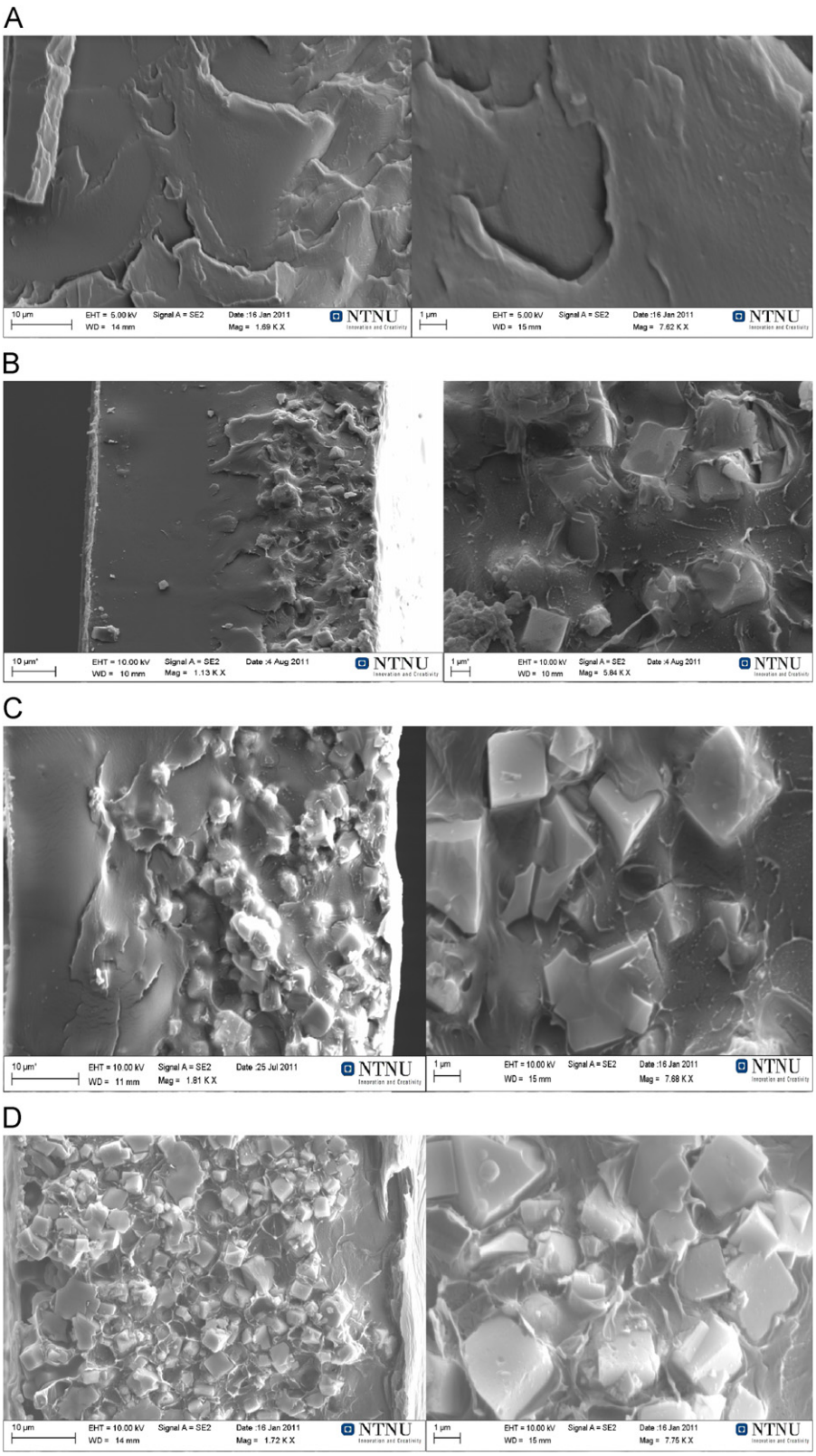

Fig. 4. FESEM images of the cross section of pure PVAc and MMMs: (A) pure PVAc, (B) PVAc+15 wt% 4A, (C) PVAc+25 wt% 4A, and (D) PVAc+35 wt% 4A.

cell used in the permeation setup is a circular stainless steel cell consisting of the top half and the bottom half, on which the feed gas inlet and low pressure outlet were designed respectively. A porous metal disk(purchased from Tridelta Siperm GmbH, Germany) placed on the circular edge of the bottom half was used to support the membrane. The membranes were masked using impermeable aluminum tape (3M 7940). Blue ribbon ashless standard filter paper with grade 589/3:2 μm size was placed between the porous metal sinter of the permeation cell and the masked membrane to protect the membrane mechanically. A wider tap with round hole in the middle of the size of membrane was put on the top to prevent leakage from feed side to permeate side. Epoxy(Alaldite 2012) was applied at the interface of the tap and membrane to prevent leakage. An O ring put on the upper flange sealed the membrane module from the exernal environment and another on the lower flange sealed the low pressure side. Further details on the construction of membrane cell can be found elsewhere [47]. A membrane with known thickness (L) is placed in the membrane cell and the system is evacuated for 24 h by a vacuum pump on both sides through a low pressure chamber denoted as LP with 100 ml capacity and high pressure chamber indicated as HP with a maximum pressure of $15 \times 100{,}000$ Pa (bar). After that the gas is allowed to pass through the membrane. The extent of gas permeating through the membrane is determined by measuring the small pressure increase (dp/dt) in the known volume (V) on the permeate side of the membrane. The permeability of gas through membrane is measured by the constant volume method from the following equation: (1)

$$\frac{P}{L} = \frac{VV_m}{ART(p_1 - p_2)} \cdot \frac{dp}{dt} \tag{1}$$

In Eq. (1), P is the permeability, V_m is the molar volume, A is the membrane area available for transport, R is the gas constant, T is the operating temperature in Kelvin and $(p_1 - p_2)$ is the pressure difference across the membrane. Area of the tested membranes was scanned and measured with scion software. The downstream pressure p_2 is much lesser than the upstream pressure p_1, so $(p_1 - p_2)$ can be replaced by p_1. To account for the leakage from outside air into the system during testing, the leakage rate is measured by evacuating the whole system for 24 h. All the valves are kept open except V_1 which is closed to ensure complete evacuation at both the high and low pressure side. After 24 h when the low pressure value reaches less than $0.01 \times 100{,}000$ Pa (mbar), membrane cell is isolated by closing valves V_2 and V_5 and the system is left for about 8 h. As the outside atmospheric pressure of air is more than $0.01 \times 100{,}000$ Pa (mbar), it will permeate (leak) into the system at a slower rate. The leakage of air into the high pressure side can be neglected due to its comparatively low value. However this is considered for the low pressure side as it can significantly effect the calculated permeability and selectivity. It is measured as $(dp/dt)_{leak}$ and subtracted from the measured pressure increase dp/dt in Eq. (2) as

$$\frac{P}{L} = \frac{VV_m}{ARTp_1}\left(\frac{dp}{dt} - \frac{dp}{dt_{leak}}\right) \tag{2}$$

The leakage rate is measured every time the membrane is mounted in the permeation setup. The ideal selectivity can then be calculated from the ratio of the single gas permeabilities. Pure PVAc and PVAc/4A MMMs with thickness from 70 μm to 90 μm having area of 2.30–2.50 cm^2 were successfully tested in the permeation setup.

3. Results and discussion

3.1. Field emission scanning electron microscopy(FESEM)

Cross sections of the PVAc and PVAc/4A MMMs were prepared by freeze-fracturing the membranes after several minutes of immersion in liquid N_2 and tested with FESEM. The results are shown in Fig. 4(A–D) with a resolution of 10 μm and 1 μm to show the dispersion of zeolite 4A within PVAc. The FESEM images show that zeolite 4A particles are uniformly distributed within PVAc without aggregation. In a 15 wt% 4A mixed matrix membrane (Fig. 4B), the dispersion of zeolite 4A particles are confined to one side of the membrane, still there is no aggregation of the

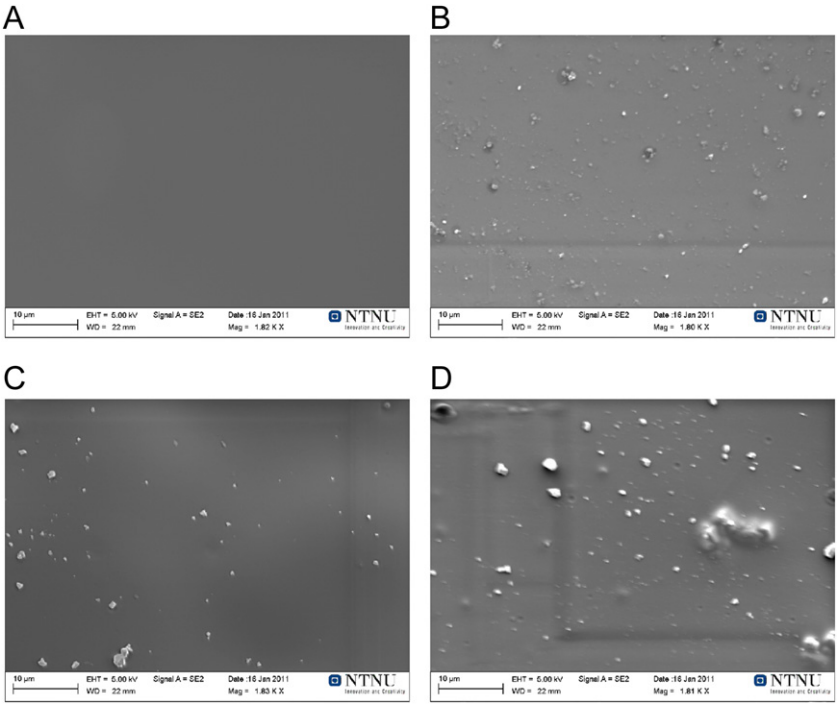

Fig. 5. FESEM images of the surface of pure PVAc and MMMs. (A) Pure PVAc, (B) PVAc+15 wt% 4A, (C) PVAc+25 wt% 4A, and (D) PVAc+35 wt% 4A.

particles visible from the image. This can be attributed to the low loading of zeolite 4A compare to the high wieght percent of polymer. As the loading of 4A particles increases to 25 wt% (C) and 35 wt% (D), the distribution of particles becomes more and more uniform across the membrane thickness. The adhesion of 4A particles with PVAc in the MMMs with 15 wt% 4A (B) and 25 wt% 4A (C) is better than in MMM with 35 wt% 4 A (D). The possible reason for this might be the high concentration of zeolite 4A in the 35 wt% 4A MMM where the applied methodology of membrane preparation is not working properly. The size of 4A particle was obtained from SEM images, which is in the range of 1–5 μm. Fig. 5 shows the surface morphology of the PVAc(A) and PVAc/4A MMMs(B–D). Zeolite 4A particles are uniformly distributed within PVAc without aggregation. The surface of MMMs is smooth which show that the casting solution was evenly spread out during membrane formation process.

3.2. X-ray diffraction

The wide angle X-ray diffraction spectra of PVAc(A), PVAc/4A MMMs(B–D) and zeolite 4A powder (E) and is presented in Fig. 6 to show the structural change in MMMs upon increasing zeolite 4A content. In general when a polymer contains large crystalline region, its WAXD spectra show sharp peaks with high intensity while broader peaks and low intensity show amorphous region [48]. Pure PVAc show a broader peak at $2\theta=15$ attributed to its semi-crystalline nature due to hydrogen bonding between the hydrogen of alkyl groups. Pure zeolite 4A show several sharp peaks while the main peak with highest intensity is around $2\theta=10$. PVAc/4A MMMs are showing both the peaks of pure PVAc and zeolite 4A, however, the intensity of both peaks are changing as the loading of zeolite 4A in the MMMs is changing. As we go from B(15 wt% 4A) toward D(35 wt% 4A), the intensity of the characteristic peak of pure PVAc i.e around $2\theta=15$ is becoming weaker and its position is slightly changing. This shows that the primary crystalline pattern in the PVAc due to hydrogen bonding between hydrogen of alkyl groups is being disrupted by the incorporation of zeolite 4A resulting in a decrease of PVAc crystallinity. As we move toward MMMs with higher zeolite 4A contents, the intensity and concentration of zeolite 4A peaks are increasing. Consequently MMMs with 15 wt% 4A (B) is more dominated by the characteristic peak of PVAc while the one with 35 wt% 4A (D) is more dominated by the peaks of zeolite 4A. This shows that the addition of zeolite 4A to the PVAc has modified its crystallinity, which is consistent with the reported literature showing similar effect [49,50]. The OH groups on the surface of 4A and hydrogen of the PVAc might have linked to form H_2 bonding [51], or strong adsorption has occurred between the zeolite 4A and PVAc in the resulting PVAc/4A MMMs [10].

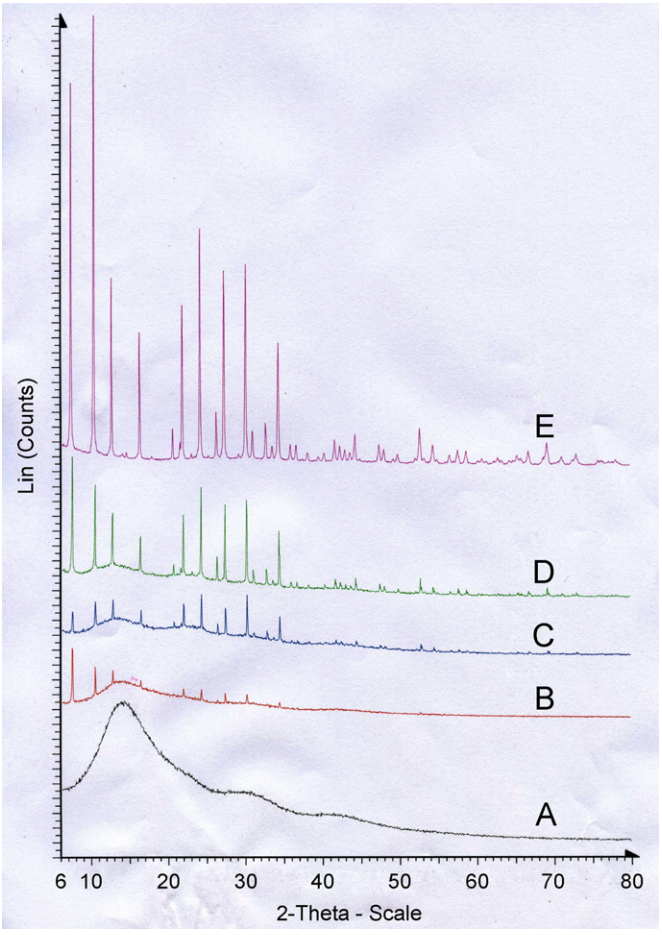

Fig. 6. X-ray diffraction spectra of Pure PVAc, zeolite 4A and MMMs: (A) pure PVAc, (B) PVAc+15 wt% 4A, (C) PVAc+25 wt% 4A, (D) PVAc+35 wt% 4A, and (E) pure zeolite 4A powder.

3.3. Differential scanning calorimetery (DSC)

DSC was carried out to understand the interaction between PVAc and zeolite 4A by finding the glass transition temperature (T_g). The results from DSC are shown in Fig. 7. The figure shows a single and clear T_g for all the membranes tested showing that the materials i.e PVAc and zeolite 4A are combined on molecular level and a new material has formed, where the properties of the individual species are no more existing. The addition of zeolite 4A upto 35 wt% to PVAc has shown a rise of 8 °C T_g, which is shown in Fig. 8. The increase of T_g obtained by the addition of zeolite/inorganic filler to the polymer has been documented by several authors in the literature. In PES–TiO_2 composite membrane, the rise of Tg with the addition of TiO_2 is caused by hydrogen bonding between the surface OH groups of TiO_2 with the sulfone or ether groups of PES [52]. Another study of CMS-Matrimid MMMs shows a rise of 15 °C in T_g and the strong adsorptive attractions between polymer and the dispersed phase has been considered for this rise [10]. The observed increase of T_g with the addition of zeolite 4A to PVAc in the current work may be either due to the strong

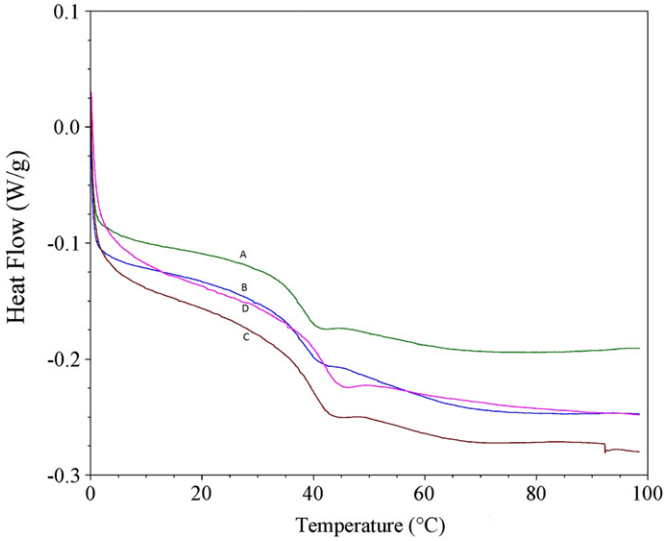

Fig. 7. DSC thermograms of pure PVAc and MMMs: (A) pure PVAc, (B) PVAc+15 wt% 4A, (C) PVAc+25 wt% 4A, and (D) PVAc+35 wt% 4A.

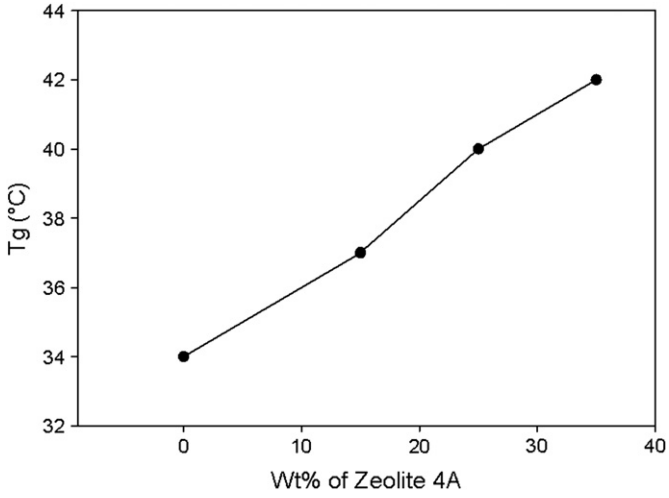

Fig. 8. Effect of zeolite 4A loading on the glass transition temperature(T_g).

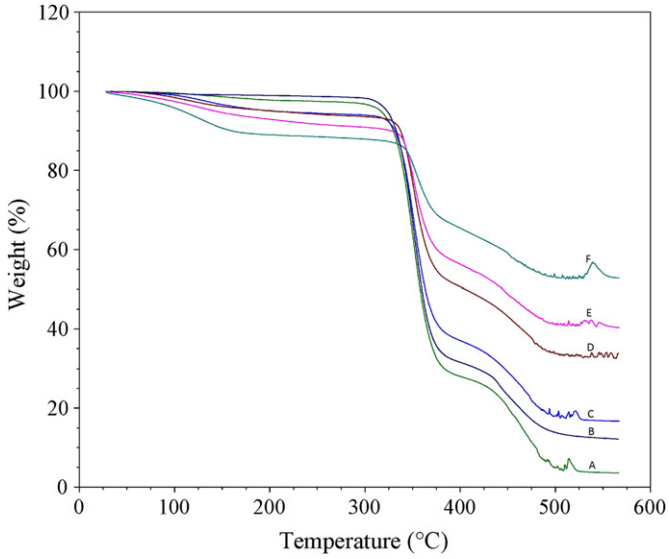

Fig. 9. TGA analyses of pure PVAc and MMMs: (A) pure PVAc, (B): PVAc+15 wt%4A, (C) PVAc+25 wt%4A, (D) PVAc+35 wt% 4A, and (E) PVAc+45 wt%4A.

adsorption characteristic of zeolite 4A or the H_2 bonding mechanism as discussed above.

3.4. Thermogravimetric analysis (TGA)

One of the challenges with the polymeric membrane is their low thermal stability to cope with the harsh process conditions of temperature and pressure. Samples of PVAc and PVAc/4A MMMs were prepared and analyzed in the TGA instrument to find the effect of zeolite particles on the thermal stability of these membranes. The obtained results are shown as weight loss vs. temperature in Fig. 9. A clear and systematic change is shown in the decomposition temperature, weight loss and residue left as we add more and more zeolite particles to the PVAc. Pure PVAc starts decomposing around 300 °C and continue to decompose till 500 °C which is consistent with the previous work [53]. As shown in Fig. 9, the decomposition of PVAc occurs in two steps such that about 70% of the material is decomposed in the first step and 25% in the second step leaving behind 5% residue. Previous work on the thermal degradation of PVAc show that the degradation occurs in two steps such that 72% in the first step and around 25% in the second step [54]. Also it is shown that acetic acid is the main product of PVAc thermal degradation [55]. As we add more and more zeolite particles to PVAc, the onset of decomposition is shifting to the right and with 45 wt% zeolite decomposition starts at 325 °C.

For the 45 wt% zeolite 4A MMMs the residue left is 55 wt%. In this 55 wt% residue 45 wt% should be zeolite 4A as it will not decompose at this temperature and the remaining 10 wt% is residue left from PVAc decomposition. This shows that the wieght percent of residue left from the degradation of PVAc has increased which was only 5 wt% in the case of pure PVAc. This increase in the residue content is important to be considered when explaining the thermal stability of the MMMs. Although the exact mechanism of the increase in PVAc residue is not known, however it may be deduced that the zeolite particles provide increase surface sites for the chemisorption of PVAc that would not be available when pure PVAc is decomposed. Both zeolite 4A and PVAc have been integrated on molecular level and a new material has been formed with improved thermal stability. DSC results showing increase of T_g upon addition of zeolite 4A to PVAc also support these results.

3.5. Separation properties

Both PVAc and PVAc/4A MMMs were used to find the single gas permeation of N_2, O_2, H_2 and CO_2 gases using in-house built permeation setup. The physical properties of the tested gases show that H_2 is the smallest and most ideal gas molecule. N_2 has the highest kinetic diameter and CO_2 is the most non ideal gas. The effects of zeolite 4A loading, operating temperature and pressure on the permeability and selectivity of the membranes were studied.

Figs. 10 and 11 show the effect of zeolite 4A loading on the permeability and selectivity of PVAc in the MMMs respectively. As the loading of zeolite 4A increases, permeability of the membranes decreases for all four gases N_2, O_2, H_2 and CO_2 with a corresponding increase in the selectivity of gas pairs O_2/N_2 (6.45 max), CO_2/N_2 (100.54 max) and H_2/N_2 (156 max). This trend of decreasing permeability with a corresponding increase in selectivity is consistent up to 25 wt% zeolite 4A; however, increasing the loading to 35 wt% resulted in almost no significant change in permeability and selectivity. It can be deduced that the applied methodology of membrane preparation is working well up to 25 wt% zeolite 4A As the loading is increased from 25 wt% to

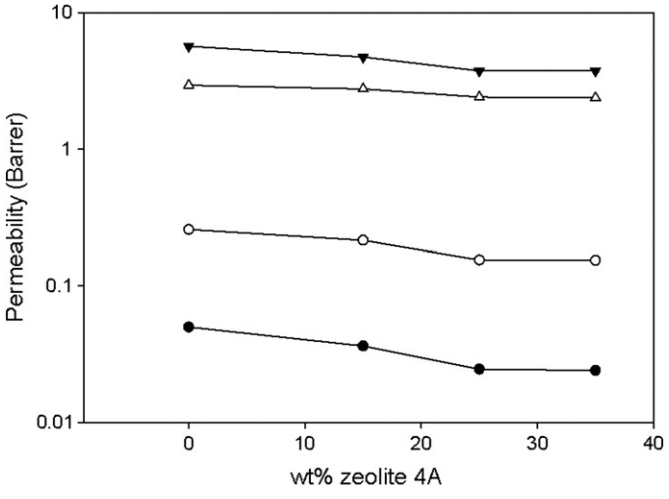

Fig. 10. Effect of zeolite 4A loading on permeability. (●) N_2, (○) O_2, (Δ) CO_2, and (▼) H_2. T=303 K, P=(8) × 100,000 Pa(bars).

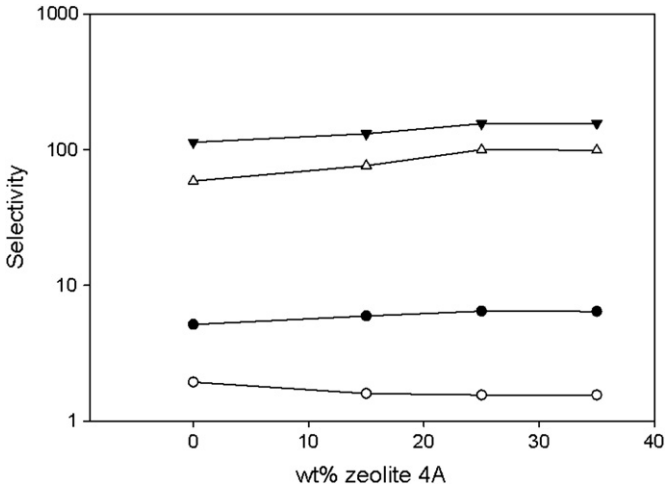

Fig. 11. Effect of zeolite 4A loading on selectivity. (●) O_2/N_2, (○) H_2/CO_2, (Δ) CO_2/N_2, and (▼) H_2/N_2. $T=303$ K, $P=(8)\times 100{,}000$ Pa(bars).

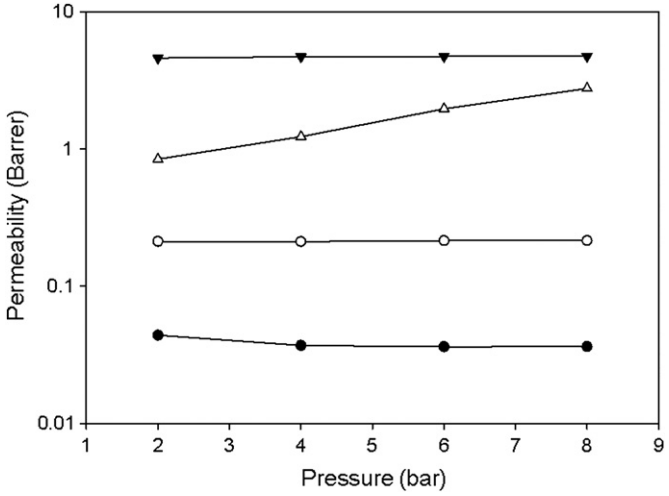

Fig. 12. Effect of feed pressure on permeability of MMM with 15 wt% 4A. (●) N_2, (○) O_2, (Δ) CO_2, and (▼) H_2. $T=303$ K.

35 wt%, some microscopic voids might have created at the interface of zeolite and PVAc as also evident from the FESEM results. The formation of these voids favor the increase of non selective permeation that counter-acts with the normal trend of increasing selectivity with a corresponding decrease in permeability and the resulting permeability and selectivity for a 35 wt% 4A MMM is almost the same as for MMM with 25 wt% 4A. This is also supported by the DSC and TGA results where the increase of T_g and reduction of residue obained upon decomposition from 15 wt% to 25 wt% is more than as compared to 25–35 wt%. According to the Maxwell equation, addition of zeolite 4A to the polymer should increase the selectivity significantly with a slight increase in the permeability. This is only possible when the available zeolite micropores are open during permeation and thinner and defect free membranes are formed. However it is a challenge in MMMs, as zeolite pores are normally clogged or partially clogged at low temperature. Also the fabrication of thinner and defect free membranes is limited by the available size of zeolite 4A in the market. Our results are consistent with the literature results that show an increase of selectivity with a corresponding decrease in permeability for most of the cases [33,40,56].

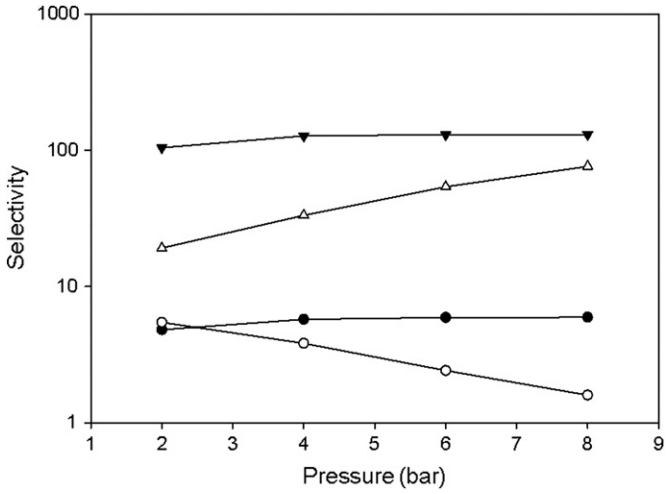

Fig. 13. Effect of feed pressure on selectivity of MMM with 15 wt% 4A. (●) O_2/N_2, (○) H_2/CO_2, (Δ) CO_2/N_2, and (▼) H_2/N_2. $T=303$ K.

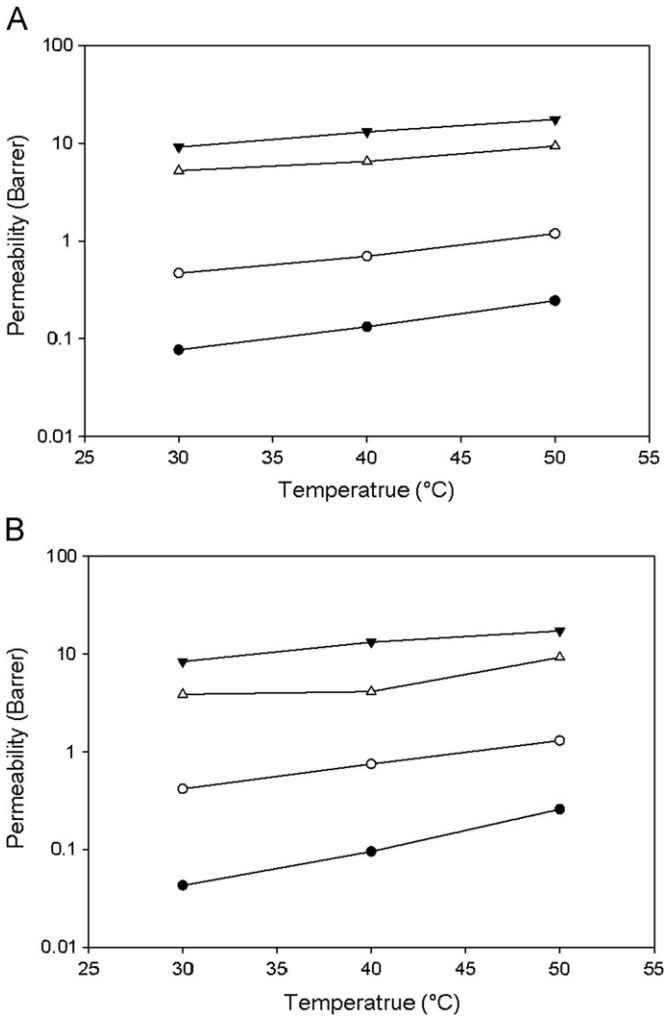

Fig. 14. Effect of operating temperature on permeability of (A) PVAc, (B) MMM with 15 wt% 4A. (●) N_2, (○) O_2, (Δ) CO_2, and (▼) H_2, $P=(8)\times 100{,}000$ Pa(bar).

The effect of operating pressure on the permeability and selectivity of MMM with 15 wt% zeolite 4A is shown in Figs. 12 and 13 respectively. As the pressure is increased from $(2)\times 100{,}000$ Pa (bars) to $(8)\times 100{,}000$ Pa (bars), H_2 permeability almost remains

constant and a slight increase is observed in the permeability of O_2. The permeability of N_2 and CO_2 is decreased and increased respectively as the pressure is increased. H_2 is the most ideal gas among the tested gas species and therefore may show little effect with change in pressure. The slight increase of O_2 and significant increase of CO_2 permeability with pressure may be attributed to their nonideal nature compare to H_2 with CO_2 being the most nonideal gas. The operating temperature of permeation i.e. 30 °C is very close to the T_g of PVAc and PVAc/4A MMMs that range from 34 °C to 42 °C. It means that although the membranes are in the glassy state at the operating temperature, still they are not rigid enough to avoid CO_2 plasticization. Reported results also show CO_2 plasticization around $10 \times 100{,}000$ Pa (bars) [57,58]. The decrease of N_2 permeability in the given pressure range can be explained on the bases of its compaction behavior as observed in the literature [59,60]. Due to this decrease of N_2 permeability with increase in pressure, the selectivity of O_2/N_2, H_2/N_2 are also increased. A more rapid rise in the CO_2/N_2 selectivity is a result of both the plasticization of CO_2 coupled with compaction behavior of N_2.

The effect of operating temperature from 30 °C (glassy) to 50 °C (rubbery) on the permeability and selectivity of PVAc and MMMs is shown in Figs. 14 and 15 respectively. As the operating temperature is increased from 30 °C to 50 °C, permeability of all the gases is increased with a maximum of $(1.19) \times 3.348 \times 10^{-19}$ kmol m/(m^2 s Pa)(barrer) for O_2, 17.55 barrer for H_2 and 9.35 barrer for CO_2 with a corresponding decrease in their selectivity over N_2. Generally permeation of a gas through dense polymeric membranes is considered an activated process which can be represented by an Arhenius type of equation, expressing the temperature dependency of the permeation parameters as follows:

$$P = P_O \exp\left(\frac{-E_p}{RT}\right) \tag{3}$$

$$D = D_O \exp\left(\frac{-E_d}{RT}\right) \tag{4}$$

$$S = S_O \exp\left(\frac{-\Delta H_s}{RT}\right) \tag{5}$$

where E_p, E_d and ΔH_s are the activation energy for permeation, diffusion and the heat of solution respectively. For small noninteracting gases such as nitrogen, helium, methane or hydrogen, the ΔH_s has a small positive value which indicates that the solubility increases slightly with increasing temperature. For large and condensable molecules the heat of sorption is negative and solubility decreases with increasing temperature [21]. A similar temperature effect on the permeability and selectivity of gas pair CO_2/N_2 has been reported for PDMS. Here the change in diffusion coefficient with temperature is almost the same for both N_2 and CO_2 and a significant difference in the increase of solubility coefficient with increase in temperature is observed, leading to decrease in the selectivity of CO_2/N_2 gas pair [60]. The activation energy for permeation E_p has a direct relation with the kinetic diameter of gas molecules. The lower activation energy of CO_2 due to its smaller kinetic diameter gives comparative higher permeability than N_2 at the same operating temprature. On the contrary, gas molecules with higher activation energy i.e. N_2 can benefit more from the temperature increase leading to decrease of CO_2/N_2 selectivity [28]. As the selectivity of all the three gas pairs O_2/N_2, H_2/N_2 and CO_2/N_2 has decreased with increase in temperature for the PVAc-4A MMMs considered here, therefore activation energy may be the best explanation for this case. The selectivity of H_2/CO_2 increases when temperature is increased from 30 °C to 40 °C and then decreases as the temperatures is further increased to 50 °C. From 30 °C to 40 °C the membrane material is in the glassy state and the increase of temperature has a small positive effect on the solubility coefficient and a more significant effect on the diffusion coefficient of permanent gas like H_2. The increase of temperature within the glassy state has a negative effect on the solubility of CO_2 and the resulting H_2/CO_2 selectivity is increased as the temperature is increased from 30 °C to

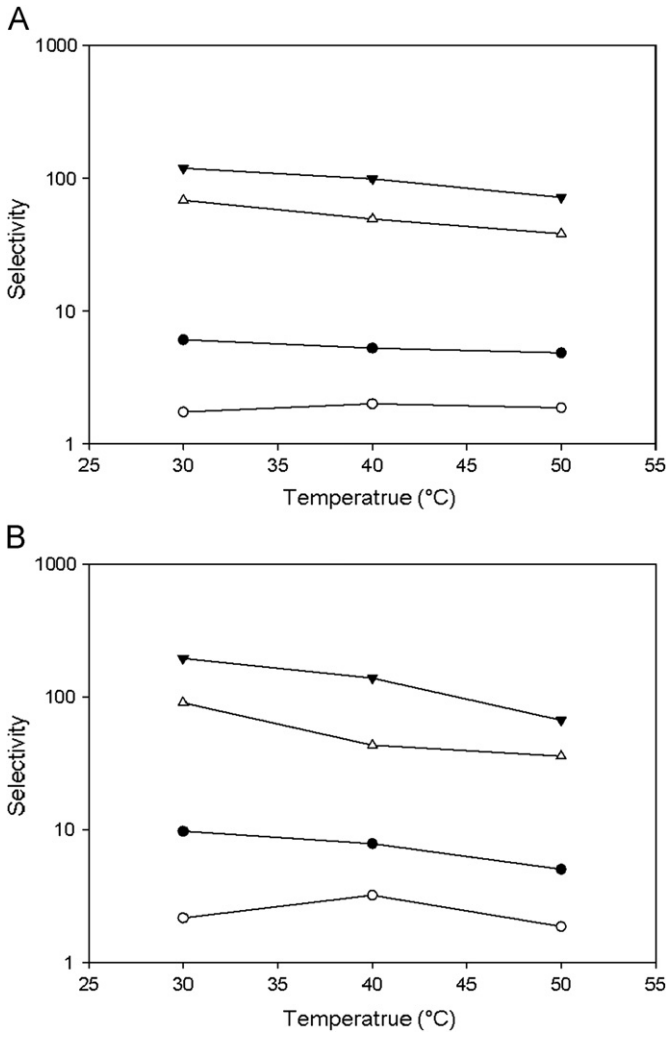

Fig. 15. Effect of operating temperature on selectivity of (A): PVAc, MMM with 15 wt% 4A. (●) O_2/N_2, (○) H_2/CO_2, (Δ) CO_2/N_2, and (▼) H_2/N_2, P=(8)(bars).

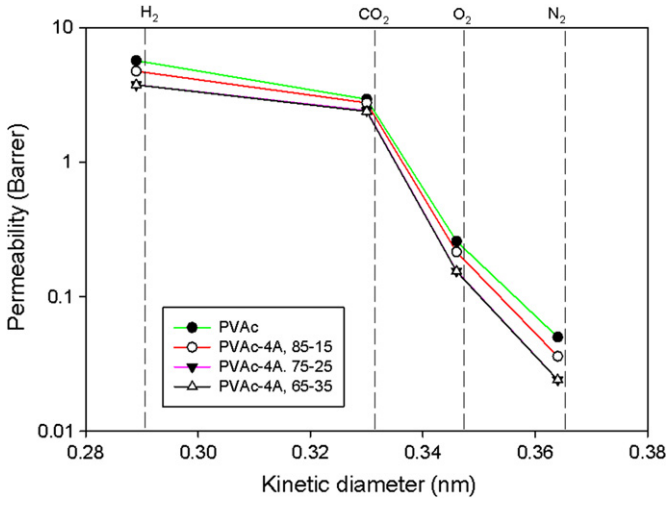

Fig. 16. Single gas permeability against the kinetic diameter of gas molecules. T=303 k, P=(8) × 100,000 Pa(bars).

Table 1
Published literature results showing advancement in MMMs along with the present results (P.R).

Polymer	Filler	P_{co_2} kmol m/ (m^2 s Pa) (barrer)	P_{N_2} kmol m/ (m^2 s Pa)(barrer)	P_{O_2} kmol m/ (m^2 s Pa)(barrer)	P_{H_2}kmol m/ (m^2 s Pa) (barrer)	$\alpha\frac{CO_2}{N_2}$	$\alpha\frac{O_2}{N_2}$	$\alpha\frac{H_2}{N_2}$	$\alpha\frac{CO_2}{CH_4}$	Refs.
PDMS	Silica,Silicalite, 5A, KY	1910	521	1370		3.66	2.62		3.0	[31]
EPDM	Silica,Silicalite, 5A, KY	55	8.50	40		6.47	4.70		4.60	[31]
PVAc	4A		0.036	0.35			9.72			[33]
PES	13X ,4A	5.20, 10.70	0.12, 0.25	0.50, 1.10	8.50, 14	43, 43	4, 4.40	71, 56		[34]
PSF	13X	6.10	0.32	1.60	14.70	19.10	5.0	46	19.0	[35]
PSF	MCM-41, Silica	20.50, 7.70	0.70, 0.23	3.80, 1.36		29.30,33.50	5.40, 5.91			[36]
Matrimid	4A, 13X,	9.36, 33.40	0.45, 1.35	1.91,6.58		20.60, 24.7	4.20, 4.87		2.2, 6.8	[37]
Matrimid+ TAP	4A	0.18	0.0018	0.033		102	18.20		617	[37]
Matrimid	4A+plastisizer		0.02, 0.15	0.20, 1.10			8.60, 7.10			[38]
PI	4A		0.03	0.37			12.50			[40]
Matrimid	C60	3.79	0.161	1.09		23.54	6.80		35	[41]
PSF	CMS		1.08	6.52			6.05			[42]
Matrimid	Carbon Aerogel	13.34	0.34	2.86	34.87	39.23	8.41	102	45.10	[43]
Matrimid	ZSM-5,MCM-48	8.65, 9.35	0.17, 0.30	1.80, 1.94	22, 23	51, 31	10.30,6.40	128,76	66,33.4	[44]
PVAc	CuTPA(MOF)	3.26	0.091	0.62		35.40	6.79		40.40	[45]
Matrimid	MOF	20.20	0.52	4.12	53.80	38.84	7.90	103.53	44.70	[62]
BPPO	CNT	129	4.30			30				[63]
PEBAX-1657	MWCNT	262	4.48	12.03	40.96	58.48	2.68	9.14		[64]
PSF	SBA-15						7.20		38.20	[65]
PI	POSS	53.86	2.37	15.61		22.72	6.60		27.20	[66]
PI	AlPO	51	2.10	18.50		24.60	8.91		40.93	[67]
PVAc	4A	2.413	0.024	0.155	3.75	100.54	6.45	156		P.R

40 °C. Further increasing the operating temperature to 50 °C is now changing the membrane material into the rubbery state. The solubility of more condensable gases like CO_2 is comparatively high in the rubbery state. Therefore the increase of temperature to 50 °C has a positive effect on the solubility of CO_2 as the material is changed from glassy to rubbery state. Permanent gases such as H_2 are compratively less permeable in the rubbery state and consequently the H_2/CO_2 selectivity comes down as the temperature is increased to 50 °C.

Comparing the effect of temperature on both the pure PVAc and MMMs with 15 wt% zeolite show that the increase in permeability of O_2 and H_2 in the MMMs is more compared to the pure polymer at the higher temperature of 40 °C and 50 °C. At the higher temperature, zeolite 4A in the MMMs may be more activated with open pores that favor increase of permeability. This supports our previous notion of clogging zeolite 4A particles at low temperature. The permeability of H_2, CO_2, O_2 and N_2 at $(8)\times 100{,}000$ Pa(bar) and 303 K is plotted against the kinetic diameter of these gases as shown in Fig. 16. It is shown that gas molecules with higher kinetic diameter has low permeability and vice versa and follow the order as $H_2 > CO_2 > O_2 > N_2$. It can be deduced that molecular sieving may be the dominant mode of transport mechanism beside solution diffusion which is an established mechanism in polymeric membranes. The gas separation properties of MMMs comprising different polymers and fillers from the published literature is shown in Table 1. The highest values of permeability and selectivity obtained by different researchers are reported and compared with the results obtained from our present work. Comparison of the results show that although higher permeability for CO_2 and H_2 are reported in the literature, a comparatively better selectivity of $CO_2/N_2 = 100.54$ and $H_2/N_2 = 156$ was obtained for pure gas permeation from our MMMs containing 75 wt% PVAc and 25 wt% zeolite 4A. Mixed gas permeation was not carried out as the setup used in our work was not designed for it. However mixed gas permeation is expected to deviate from the pure gas permeation to some extent. In multicomponent mixture the permeation of each species is affected by the presence of other in the mixture both through thermodynamic interaction and coupling phenomena. This is more pronounced in the case of liquid mixtures as compared to gas mixures. Coupling phenomena may either positively or negatively effect the permeation of mixed gas stream. However, the Coupling phenomena are difficult to describe, predict or even measure quantitatively [21]. Literature study shows that the selectivity of gas pairs CO_2/N_2 and CO_2/CH_4 decreases in the mixed gas permeation [60,61]. The solubility selectivity is shown to be more affected in the mixed gas permeation as compared to the diffusivity selectivity giving comparatively less permselectivity. However, the importance of obtained higher selectivity in the present work for single gas permeation cannot be disregarded when compared with the reported results.

The low permeance obtained in the current work can be improved by preparing thinner membranes. The thickness of our membranes are in the range from 70 μm to 90 μm, and reducing it to about 50 μm may be possible by using zeolite 4A particles with size around 1 μm or even less than 1 μm. Also the clogging of zeolite pores may be investigated and its preheat treatment at different temperature may be helpful to improve the permeability.

4. Conclusion

Pure PVAc and PVAc-4A MMMs were prepared using dichloromethane as a solvent and the solution casting method. The membranes were characterized by optical microscope, FESEM, DSC, TGA, XRD and single gas permeation. FESEM results show that zeolite 4A particles are homogeneously dispersed up to 35 wt% within the polymer without aggregation and defect free membranes in the range of 70–90 μm were formed. The thermal stability of PVAc is improved and a rise of 8 °C in the T_g is achieved by the addition of zeolite 4A in the resulting MMMs as shown by the DSC and TGA results. The addition of zeolite 4A to PVAc has decreased its primary crystallinity possibly by

disrupting its molecules. New hydrogen bondings may be formed between 4A and PVAc and the overall crystallinity is modified. In single gas permeation, the effect of zeolite 4A loading, operating temperature and pressure were investigated. The obtained results show that the addition of zeolite 4A upto 25 wt% has increased the selectivity of gas pairs O_2/N_2, H_2/N_2 and CO_2/N_2 by 25%, 37% and 70% respectively with a corresponding decrease in their permeabilities. As the operating temperature was increased from 30 °C to 50 °C, permeability of all the gases was increased with a maximum of $(1.19)\times 3.348\times 10^{-19}$ kmol m/(m^2 s Pa)(barrer) for O_2, $(17.55)\times 3.348\times 10^{-19}$ kmol m/(m^2 s Pa) (barrer) for H_2 and $(9.35)\times 3.348\times 10^{-19}$ kmol m/(m^2 s Pa) (barrer) for CO_2 with a corresponding decrease in their selectivity over N_2. As the pressure is increased from $(2)\times 100{,}000$ Pa(bars) to $(8)\times 100{,}000$ Pa(bars), the permeability of H_2 almost remains constant and slightly increases for O_2. Permeability of N_2 and CO_2 is decreased and increased respectively leading to increased selectivity of CO_2/N_2 as well as H_2/N_2 and O_2/N_2. The obtained results are consistent with the reported literature data.

Acknowledgments

The authors want to thank Prof. Halvard Svendsen for financial support through the CCERT Project (through Norwegian Research Council).

Nomenclature

PVAc	polyvinyl Acetate
MMMs	mixed matrix membranes
FESEM	field emission scanning Electron microscope
DSC	differential scanning calorimetory
TGA	thermogravimetric analysis
XRD	X-ray diffraction
Tg	glass transition temperature
UOP	universal oil products
CMS	carbon molecular sieves
CMSMs	carbon molecular sieve membranes
PI	polyimide
ASGE	advanced speciality gas equipment
DCM	dichloromethane
M.wt	molecular weight
ppm	parts per million
LP	low pressure chamber
HP	high pressure chamber
P	permeability
V_m	molar volume
A	membrane area
R	universal gas constant
p_1	upstream pressure
p_2	downstream pressure
T	operating temperature
V	known volume on the permeate side
L	thickness of membrane
WAXD	wide angle X-ray diffraction
PDMS	polydimethylsiloxane
P	permeability coefficient
P_O	pre-exponential term in permeability
D	diffusion coefficient
D_O	pre-exponential term in Diffusion
S	solubility Coefficient
S_O	pre-exponential term in solubility
E_d	activation energy for diffusion
E_p	activation energy for permeation
ΔH_s	heat of solution
EPDM	ethylene propylene diene monomer
PES	polyethersulfone
PSF	polysulfone
TAP	2,4,6- triaminopyrimide
MOF	metal organic framework
BPPO	brominated poly (2, 6-diphenyl-1, 4-phenylene oxide)
CNT	carbon nanotubes
PEBAX-1657	poly (ether-block-amide)
MWCNT	multiwalled carbon nanotubes
POSS	polyhedral oligomeric silsesquioxanes
AIPO	layered aluminophosphate

References

[1] F. Barbir, T.N. Veziroğlu, H.J. Plass Jr, Environmental damage due to fossil fuels use, Int. J. Hydrogen Energy 15 (1990) 739–749.
[2] D. Aaron, C. Tsouris, Separation of CO_2 from flue gas: a review, Sep. Sci. Technol. 40 (2005) 321–348.
[3] E.K. Lee, W.J. Koros, Membranes, synthetic, applications, in: R.A. Mayers (Ed.), Encylopedia of Physcial Science and Technology, Academic Press, New York, 2002, pp. 279–345.
[4] T.-J. Kim, B. Li, M.-B. Hägg, Novel fixed-site-carrier polyvinylamine membrane for carbon dioxide capture, J. Polym. Sci. Part B: Polym. Phys. 42 (2004) 4326–4336.
[5] R.W. Baker, Future .directions of membrane gas separation technology, Ind. Eng. Chem. Res. 41 (2002) 1393–1411.
[6] A.G. Fane, R. Wang, Y. Jia, Membrane technology: ast, present and future membrane and desalination technologies, in: L.K. Wang, J.P. Chen, Y.-T. Hung, N.K. Shammas (Eds.), Handbook of Environmental Engineering, Humana Press, NY, US. 2008, pp. 1–45.
[7] P.K. Gantzel, U. Merten, Gas separations with high-flux cellulose acetate membranes, Ind. Eng. Chem. Des. Dev. 9 (1970) 331–332.
[8] W.J. Koros, G.K. Fleming, Membrane-based gas separation, J. Memb. Sci. 83 (1993) 1–80.
[9] S.A. Stern, Polymers for gas separations: the next decade, J. Memb. Sci. 94 (1994) 1–65.
[10] D.Q. Vu, W.J. Koros, S.J. Miller, Mixed matrix membranes using carbon molecular sieves: preparation and experimental results, J. Memb. Sci. 211 (2003) 311–334.
[11] L.M. Robeson, Correlation of separation factor versus permeability for polymeric membranes, J. Memb. Sci. 62 (1991) 165–185.
[12] W.J. Koros, M.R. Coleman, D.R.B. Walker, controlled permeability polymer membranes, Annu. Rev. Mater. Sci. 22 (1992) 47–89.
[13] C.M. Zimmerman, W.J. Koros, Polypyrrolones for membrane gas separations. structural comparison of gas transport and sorption properties, J. Polym. Sci. Part B: Polym. Phys. 37 (1999) 1235–1249.
[14] F. Hamad, T. Matsuura, Performance of gas separation membranes made from sulfonated brominated high molecular weight poly(2,4-dimethyl-l,6-phenylene oxide), J. Memb. Sci. 253 (2005) 183–189.
[15] T. Mizumoto, T. Masuda, T. Higashimura, Polymerization of [o-(trimethylgermyl)phenyl] acetylene and polymer characterization, J. Polym. Sci. Part A: Polym. Chem. 31 (1993) 2555–2561.
[16] C.J. Orme, M.K. Harrup, T.A. Luther, R.P. Lash, K.S. Houston, D.H. Weinkauf, F.F. Stewart, Characterization of gas transport in selected rubbery amorphous polyphosphazene membranes, J. Memb. Sci. 186 (2001) 249–256.
[17] G. Polotskaya, M. Goikhman, I. Podeshvo, V. Kudryavtsev, Z. Pientka, L. Brozova, M. Bleha, Gas transport properties of polybenzoxazinoneimides and their prepolymers, Polymer 46 (2005) 3730–3736.
[18] K. Tanaka, M.N. Islam, M. Kido, H. Kita, K.-I. Okamoto, Gas permeation and separation properties of sulfonated polyimide membranes, Polymer 47 (2006) 4370–4377.
[19] L.M. Robeson, The upper bound revisited, J. Memb. Sci. 320 (2008) 390–400.
[20] M.J. Muñoz-Aguado, M. Gregorkiewitz, Preparation of silica-based microporous inorganic gas separation membranes, J. Memb. Sci. 111 (1996) 7–18.
[21] M. Mulder, Basic Principles of Membrane Technology, Kluwer Academic Publishers, Dordrecht, Netherland, 2003.
[22] K. Kusakabe, T. Kuroda, S. Morooka, Separation of carbon dioxide from nitrogen using ion-exchanged faujasite-type zeolite membranes formed on porous support tubes, J. Memb. Sci. 148 (1998) 13–23.
[23] D.Q. Vu, W.J. Koros, S.J. Miller, High pressure CO_2/CH_4 separation using carbon molecular sieve hollow fiber membranes, Ind. Eng. Chem. Res. 41 (2001) 367–380.
[24] Y. Xiao, Y. Dai, T.-S. Chung, M.D. Guiver, Effects of brominating matrimid polyimide on the physical and gas transport properties of derived carbon membranes, Macromolecules 38 (2005) 10042–10049.

[25] G. Saracco, H.W.J.P. Neomagus, G.F. Versteeg, W.P.M.VPlease check the edits made in the author name and correct if necessary. Swaaij, High-temperature membrane reactors: potential and problems, Chem. Eng. Sci. 54 (1999) 1997–2017.
[26] J. Caro, M. Noack, P. Kölsch, R. Schäfer, Zeolite membranes—state of their development and perspective, Microporous Mesoporous Mat. 38 (2000) 3–24.
[27] J.A. Lie, M.-B. Hägg, Carbon membranes from cellulose and metal loaded cellulose, Carbon 43 (2005) 2600–2607.
[28] X. He, J.A. Lie, E. Sheridan, M.-B. Hägg, Preparation and characterization of hollow fiber carbon membranes from cellulose acetate precursors, Ind. Eng. Chem. Res. 50 (2011) 2080–2087.
[29] D.R. Paul, D.R. Kemp, The diffusion time lag in polymer membranes containing adsorptive fillers, J. Polym. Sci. Pol. Sym. 41 (1973) 79–93.
[30] S. Kulprathipanja, R.W. Neuzil, N.N. Li, Separation of Fluids by Means of Mixed Matrix Membranes, US Patent 4740219, 1988.
[31] J.-M. Duval, B. Folkers, M.H.V. Mulder, G. Desgrandchamps, C.A. Smolders, Adsorbent filled membranes for gas separation. Part 1. improvement of the gas separation properties of polymeric membranes by incorporation of microporous adsorbents, J. Memb. Sci. 80 (1993) 189–198.
[32] Ş.B. Tantekin-Ersolmaz, Ç. Atalay-Oral, M. Tatlıer, A. Erdem-Şenatalar, B. Schoeman, J. Sterte, Effect of zeolite particle size on the performance of polymer–zeolite mixed matrix membranes, J. Memb. Sci. 175 (2000) 285–288.
[33] R. Mahajan, W.J. Koros, Factors controlling successful formation of mixed-matrix gas separation materials, Ind. Eng. Chem. Res. 39 (2000) 2692–2696.
[34] M.G. Süer, N. Baç, L. Yilmaz, Gas permeation characteristics of polymer–zeolite mixed matrix membranes, J. Memb. Sci. 91 (1994) 77–86.
[35] T.M. Gür, Permselectivity of zeolite filled polysulfone gas separation membranes, J. Memb. Sci. 93 (1994) 283–289.
[36] B.D. Reid, F.A. Ruiz-Trevino, I.H. Musselman, K.J. Balkus, J.P. Ferraris, Gas permeability properties of polysulfone membranes containing the mesoporous molecular sieve MCM-41, Chem. Mater. 13 (2001) 2366–2373.
[37] H.H. Yong, H.C. Park, Y.S. Kang, J. Won, W.N. Kim, Zeolite-filled polyimide membrane containing 2,4,6-triaminopyrimidine, J. Memb. Sci. 188 (2001) 151–163.
[38] R. Mahajan, R. Burns, M. Schaeffer, W.J. Koros, Challenges in forming successful mixed matrix membranes with rigid polymeric materials, J. Appl. Polym. Sci. 86 (2002) 881–890.
[39] R. Mahajan, W.J. Koros, Mixed matrix membrane materials with glassy polymers, Polym. Eng. Sci. 42 (2002) 1420–1431.
[40] R. Mahajan, W.J. Koros, Mixed matrix membrane materials with glassy polymers, Polym. Eng. Sci. 42 (2002) 1432–1441.
[41] T.-S. Chung, S.S. Chan, R. Wang, Z. Lu, C. He, Characterization of permeability and sorption in Matrimid/C60 mixed matrix membranes, J. Memb. Sci. 211 (2003) 91–99.
[42] W.A.W. Rafizah, A.F. Ismail, Effect of carbon molecular sieve sizing with poly(vinyl pyrrolidone) K-15 on carbon molecular sieve–polysulfone mixed matrix membrane, J. Memb. Sci. 307 (2008) 53–61.
[43] Y. Zhang, I.H. Musselman, J.P. Ferraris, K.J. Balkus, Gas permeability properties of mixed-matrix matrimid membranes containing a carbon aerogel: a material with both micropores and mesopores, Ind. Eng. Chem. Res. 47 (2008) 2794–2802.
[44] Y. Zhang, K.J. Balkus Jr., I.H. Musselman, J.P. Ferraris, Mixed-matrix membranes composed of Matrimid® and mesoporous ZSM-5 nanoparticles, J. Memb. Sci. 325 (2008) 28–39.
[45] R. Adams, C. Carson, J. Ward, R. Tannenbaum, W. Koros, Metal organic framework mixed matrix membranes for gas separations, Microporous Mesoporous Mater. 131 (2010) 13–20.
[46] I.F.J. Vankelecom, E. Merckx, M. Luts, J.B. Uytterhoeven, Incorporation of zeolites in polyimide membranes, J. Phys. Chem. 99 (1995) 13187–13192.
[47] D. Grainger, Development of Carbon Membranes for Hydrogen Recovery, Ph.D. Thesis vol.2007:195, Department of Chemical Engineering, NTNU, Trondheim, 2007.
[48] J.H. Kim, Y.M. Lee, Gas permeation properties of poly(amide-6-b-ethylene oxide)–silica hybrid membranes, J. Memb. Sci. 193 (2001) 209–225.
[49] X. Tong-Hu, X. Xiao-Li, Q. Hai-Jiao, Y. Xiao-Gang, Z. Rui-Feng, Zeolite 4A-incorporated polymeric membranes for pervaporation separation of methanol–methyl acetate mixtures, J. Inorg. Organomet. Polym. Mater. (2011) 1–7.
[50] M.I. Ahmad, S.M.J. Zaidi, S.U. Rahman, Proton conductivity and characterization of novel composite membranes for medium-temperature fuel cells, Desalination 193 (2006) 387–397.
[51] Z.-L. Xu, L.-Y. YU, L.-F. Han, Polymer–nanoinorganic particles composite membranes: a brief overview, Front. Chem. Eng. Chin. 3 (2009) 318–329.
[52] J.-F. Li, Z.-L. Xu, H. Yang, L.-Y. Yu, M. Liu, Effect of TiO_2 nanoparticles on the surface morphology and performance of microporous PES membrane, Appl. Surf. Sci. 255 (2009) 4725–4732.
[53] N. Grassie, I.F. McLean, I.C. McNeill, Thermal degradation of vinyl chloride–vinyl acetate copolymers— bulk degradation studies by thermal volatilization analysis, Eur. Polym. J. 6 (1970) 679–686.
[54] J. Blazavska-Gilev, D. Spaseska, Thermal Degradation of PVAc, J. Univ. Chem. Technol. Metall. 40 (2005) 287–290.
[55] B.B. Troitskii, G.A. Razuvaev, L.V. Khokhlova, G.N. Bortnikov, On the mechanism of the thermal degradation of polyvinyl acetate, **J.** Polym. Sci. Pol. Sym. 42 (1973) 1363–1375.
[56] G. Clarizia, C. Algieri, E. Drioli, Filler–polymer combination: a route to modify gas transport properties of a polymeric membrane, Polymer 45 (2004) 5671–5681.
[57] Y. Li, T.-S. Chung, S. Kulprathipanja, Novel Ag+-zeolite/polymer mixed matrix membranes with a high CO_2/CH_4 selectivity, A.I.Ch.E J. 53 (2007) 610–616.
[58] R.T. Adams, J.S. Lee, T.-H. Bae, J.K. Ward, J.R. Johnson, C.W. Jones, S. Nair, W.J. Koros, CO_2–CH_4 permeation in high zeolite 4A loading mixed matrix membranes, J. Memb. Sci. 367 (2011) 197–203.
[59] W.J. Koros, M.W. Hellums, Transport properties, in: J.I. Kroschwitz (Ed.), Concise Encylopedia of Polymer Science and Engineering, Wiley Interscience Publishers, New York, 1989, pp. 725–802.
[60] C.K. Yeom, S.H. Lee, J.M. Lee, Study of transport of pure and mixed CO_2/N_2 gases through polymeric membranes, J. Appl. Polym. Sci. 78 (2000) 179–189.
[61] M. Sadrzadeh, M. Amirilargani, K. Shahidi, T. Mohammadi, Pure and mixed gas permeation through a composite polydimethylsiloxane membrane, Polym. Adv. Technol. 22 (2011) 586–597.
[62] E.V. Perez, K.J. Balkus Jr., J.P. Ferraris, I.H. Musselman, Mixed-matrix membranes containing MOF-5 for gas separations, J. Memb. Sci. 328 (2009) 165–173.
[63] H. Cong, J. Zhang, M. Radosz, Y. Shen, Carbon nanotube composite membranes of brominated poly(2,6-diphenyl-1,4-phenylene oxide) for gas separation, J. Memb. Sci. 294 (2007) 178–185.
[64] R.S. Murali, S. Sridhar, T. Sankarshana, Y.V.L. Ravikumar, Gas permeation behavior of Pebax-1657 nanocomposite membrane incorporated with multi-walled carbon nanotubes, Ind. Eng. Chem. Res. 49 (2010) 6530–6538.
[65] A. Jomekian, M. Pakizeh, M. Poorafshari, S.A.A. Mansoori, Synthesis and characterization of novel modified SBA-15/PSF nanocomposite membrane coated by PDMS for gas separation, J. Nanotechnol. Eng. Med. 2 (2011) 021003.
[66] B. Dasgupta, S.K. Sen, S. Banerjee, Aminoethylaminopropylisobutyl POSS—polyimide nanocomposite membranes and their gas transport properties, Mater. Sci. Eng. B 168 (2010) 30–35.
[67] H.-K. Jeong, W. Krych, H. Ramanan, S. Nair, E. Marand, M. Tsapatsis, Fabrication of polymer/selective-Flake nanocomposite membranes and their use in gas separation, Chem. Mater. 16 (2004) 3838–3845.